Am J Physiol Renal Physiol 285: F532–F539, 2003.
First published May 20, 2003; 10.1152/ajprenal.00128.2003.

Chronic acidosis-induced alteration in bone bicarbonate and phosphate

David A. Bushinsky,[1] Susan B. Smith,[1] Konstantin L. Gavrilov,[2] Leonid F. Gavrilov,[2] Jianwei Li,[2] and Riccardo Levi-Setti[2]

[1]*Nephrology Unit, Department of Medicine, University of Rochester School of Medicine, Rochester, New York 14642; and* [2]*Department of Physics, Enrico Fermi Institute, University of Chicago, Chicago, Illinois 60637*

Submitted 1 April 2003; accepted in final form 11 May 2003

Bushinsky, David A., Susan B. Smith, Konstantin L. Gavrilov, Leonid F. Gavrilov, Jianwei Li, and Riccardo Levi-Setti. Chronic acidosis-induced alteration in bone bicarbonate and phosphate. *Am J Physiol Renal Physiol* 285: F532–F539, 2003. First published May 20, 2003; 10.1152/ajprenal.00128.2003.—Chronic metabolic acidosis increases urinary calcium excretion without altering intestinal calcium absorption, suggesting that bone mineral is the source of the additional urinary calcium. In vivo and in vitro studies have shown that metabolic acidosis causes a loss of mineral calcium while buffering the additional hydrogen ions. Previously, we studied changes in femoral, midcortical ion concentrations after 7 days of in vivo metabolic acidosis induced by oral ammonium chloride. We found that, compared with mice drinking only distilled water, ammonium chloride induced a loss of bone sodium and potassium and a depletion of mineral HCO_3^- and phosphate. There is more phosphate than carbonate in neonatal mouse bone. In the present in vitro study, we utilized a high-resolution scanning ion microprobe with secondary ion mass spectroscopy to test the hypothesis that chronic acidosis would decrease bulk (cross-sectional) bone phosphate to a greater extent than HCO_3^- by localizing and comparing changes in bone HCO_3^- and phosphate after chronic incubation of neonatal mouse calvariae in acidic medium. Calvariae were cultured for a total of 51 h in medium acidified by a reduction in HCO_3^- concentration ($[HCO_3^-]$; pH ~7.14, $[HCO_3^-]$ ~13) or in control medium (pH ~7.45, HCO_3^- ~26). Compared with incubation in control medium, incubation in acidic medium caused no change in surface total phosphate but a significant fall in cross-sectional phosphate, with respect to the carbon-carbon bond (C_2) and the carbon-nitrogen bond (CN). Compared with incubation in control medium, incubation in acidic medium caused no change in surface HCO_3^- but a significant fall in cross-sectional HCO_3^- with respect to C_2 and CN. The fall in cross-sectional phosphate was significantly greater than the fall in cross-sectional HCO_3^-. The fall in phosphate indicates release of mineral phosphates, and the fall in HCO_3^- indicates release of mineral HCO_3^-, both of which would be expected to buffer the additional protons and help restore the pH toward normal. Thus a model of chronic acidosis depletes bulk bone proton buffers, with phosphate depletion exceeding that of HCO_3^-.

ion microprobe; calcium; proton; metabolic acidosis

IN HUMANS AND OTHER MAMMALS, chronic metabolic acidosis increases urinary calcium excretion (19, 52), secondary to a direct reduction of renal tubular calcium reabsorption (67), without increasing intestinal calcium absorption (43), resulting in a net negative calcium balance (2, 49, 51). Because the vast majority of body calcium is located within the mineral stores of bone (29), the negative calcium balance implies loss of bone mineral (64). In vivo studies have shown that metabolic acidosis, induced by ammonium chloride, leads to a loss of bone mineral (3) and that patients with proximal renal tubular acidosis are shorter in height and have decreased radial bone densities and thinner iliac cortices than unaffected relatives (50). Patients with distal renal tubular acidosis also have decreased bone density and bone formation rate (38); both parameters improve after a year of HCO_3^- treatment (39). During the ongoing metabolic acidosis of chronic renal failure, blood pH can remain stable, although substantially reduced, despite progressive hydrogen ion (proton) retention, suggesting the availability of large stores of proton buffers (59). Given its large mass of potential proton buffers, bone is an obvious site for proton buffering during metabolic acidosis (12).

An in vitro model of metabolic acidosis, produced by a decrement in medium HCO_3^- concentration ($[HCO_3^-]$), induces a marked efflux of calcium from cultured neonatal mouse calvariae (11, 22, 24, 30, 36, 48), whereas metabolic alkalosis induces an influx of calcium into bone (13). During short-term (3 h) cultures, this acid-induced calcium efflux appears due to physicochemical bone mineral dissolution (24, 36). However, over longer time periods (>24 h), the calcium efflux from bone appears, in addition, due to cell-mediated bone resorption (11, 22, 30, 48). We have shown that metabolic acidosis leads to an increase in osteoclastic β-glucuronidase activity and a decrease in osteoblastic collagen synthesis (11, 42, 48). In addition, acidosis inhibits the stimulation of some, but not all, immediate early response genes (42) and reversibly inhibits expression of certain extracellular matrix genes (40). This cell-mediated resorption is a result of increased prostaglandin

Address for reprint requests and other correspondence: D. A. Bushinsky, Univ. of Rochester School of Medicine and Dentistry, Strong Memorial Hospital, 601 Elmwood Ave., Box 675, Rochester, NY 14642 (E-mail: David_Bushinsky@URMC.Rochester.edu).

The costs of publication of this article were defrayed in part by the payment of page charges. The article must therefore be hereby marked "*advertisement*" in accordance with 18 U.S.C. Section 1734 solely to indicate this fact.

E_2 synthesis, which stimulates osteoclastic resorption and suppresses osteoblastic function (31, 44, 47, 58). In vitro metabolic acidosis causes the release of mineral potassium and sodium (21, 28, 36, 37) and a depletion of mineral carbonate (26, 27), HCO_3^-, and phosphate (34).

Previously, we studied changes in midcortical ion concentrations after 7 days of in vivo metabolic acidosis induced by oral ammonium chloride (15). We found that, compared with mice drinking only distilled water, the ammonium chloride induced a loss of bone sodium and potassium and a depletion of mineral HCO_3^- and phosphate. In the previous study, we questioned whether there were regional differences in the response of mineral HCO_3^- and phosphate to acute and chronic metabolic acidosis. We have shown that acute metabolic acidosis induces a depletion of surface, but not cross-sectional, HCO_3^-, and cross-sectional, but not surface, phosphate (34). There was depletion of HCO_3^- in preference to phosphate on the bone surface and depletion of phosphate in preference to HCO_3^- in the interior of bone. The effects of acid medium on bone during acute metabolic acidosis are due to physicochemical dissolution of the mineral (24, 36), while during more chronic acidosis the effects are, in addition, due to cell-mediated resorption (9, 11, 30, 31, 40, 48). Given that physicochemical bone dissolution has very different effects on bone sodium and calcium release than cell-mediated resorption (22), we suspected that a model of chronic acidosis would alter the proton buffers in the mineral differently than for acute acidosis. As the ratio of carbonate to phosphate in mouse calvariae 3 and 7 days postnatal is ~0.12 (63), indicating that there is far more phosphate than HCO_3^- available to buffer the additional protons during metabolic acidosis, we would also suspect that an acidic medium would decrease bulk (cross-sectional) bone phosphate to a greater extent than bone carbonate.

Thus in the present study we utilized a high-resolution scanning ion microprobe with secondary ion mass spectroscopy (SIMS) to test the hypothesis that chronic acidosis would decrease bulk (cross-sectional) bone phosphate to a greater extent than bone carbonate by localizing and comparing the changes in bone HCO_3^- and phosphate after chronic incubation of neonatal mouse calvariae in an acidic medium. We found that chronic acidosis induced a fall in both cross-sectional HCO_3^- and phosphate with no change in surface HCO_3^- and phosphate and the fall in phosphate predominated over the fall in HCO_3^-. Depletion of these proton buffers, HCO_3^- and phosphate, would help to mitigate the reduction in pH during chronic acidosis.

METHODS

Organ culture of bone. Neonatal (4- to 6-day-old) CD-1 mice (Charles River, Wilmington, MA) were killed, their calvariae were removed by dissection, the adherent cartilaginous material was trimmed, and the periosteum was left intact (8, 9, 11, 13, 21–28, 30–34, 36, 37, 40–42, 46–48, 60). Exactly 2.8 ml of Dulbecco's modified Eagle's medium (M. A. Bioproducts, Walkersville, MD) containing heat-inactivated horse serum (15%), heparin sodium (10 U/ml), and penicillin potassium (100 U/ml) were preincubated at a P_{CO_2} of 40 Torr at 37°C for 3 h in 35-mm dishes (8, 9, 11, 13, 21–28, 30–34, 36, 37, 40–42, 46–48, 60). We found that 3 h are sufficient for P_{CO_2} equilibration between the incubator and the medium (25). After preincubation, 1 ml of medium was removed to determine initial medium pH and P_{CO_2} and total calcium concentration and two calvariae were placed in each dish on a stainless steel wire grid. Total bone content in each culture was controlled by using pups that were the same age and size, by using a standardized dissection procedure, and by placing two bones in each dish. Experimental and control cultures were performed in parallel and in random order.

Experimental groups. Calvariae were incubated for 51 h in either control (Ctl) or acidic (Acid) medium. In the Ctl group, the calvariae were cultured in a neutral-pH medium (pH ~7.45, $[HCO_3^-]$ ~26 meq/l). In the Acid group, the calvariae were cultured in medium in which the pH was lowered (pH ~7.14, $[HCO_3^-]$ ~13 meq/l) by the addition of 10 μl of 2.4 M HCl/ml medium to lower $[HCO_3^-]$ (Table 1). We have previously shown that calvariae are viable and exhibit similar [^{3}H]proline incorporation whether they are cultured for up to 120 h under conditions of physiological pH or of metabolic acidosis (9). Calvariae were incubated for a total of 51 h. Bones were transferred to fresh preincubated medium at 24 and 48 h. Before and after each incubation, the medium was immediately analyzed for pH, P_{CO_2}, and calcium. Fifty-one hours of incubation were chosen to represent chronic acidosis

Table 1. *Medium ion concentrations and fluxes*

		Initial				Final		
	n	pH	P_{CO_2}, Torr	$[HCO_3^-]$, mM	Ca, mg/dl	pH	P_{CO_2}, Torr	$[HCO_3^-]$, mM
0-24 h								
Ctl	12	7.46 ± 0.00	37.3 ± 0.3	26.3 ± 0.2	7.49 ± 0.03	7.27 ± 0.01	38.9 ± 0.3	17.4 ± 0.4
Acid	11	7.14 ± 0.02*	36.8 ± 0.3	13.2 ± 0.3*	7.55 ± 0.04	6.94 ± 0.03*	38.0 ± 0.4	8.1 ± 0.5*
24-48 h								
Ctl	12	7.45 ± 0.00	37.8 ± 0.2	26.0 ± 0.0	7.49 ± 0.02	7.22 ± 0.01	39.7 ± 0.4	15.7 ± 0.6
Acid	11	7.14 ± 0.01*	37.3 ± 0.2	12.1 ± 0.3*	7.55 ± 0.03	6.89 ± 0.02*	39.0 ± 0.4	7.0 ± 0.4*
48-51 h								
Ctl	12	7.45 ± 0.0	38.5 ± 0.5	26.0 ± 0.1	7.58 ± 0.04	7.41 ± 0.00	39.2 ± 0.4	24.2 ± 0.3
Acid	11	7.15 ± 0.00*	38.4 ± 0.6	12.9 ± 0.3*	7.60 ± 0.03	7.10 ± 0.01*	39.0 ± 0.4	11.7 ± 0.4*

Values are means ± SE. *n,* No. of pairs of calvariae in each group. Pairs of calvariae were incubated for 51 h in either control (Ctl) or acidic (Acid) medium. In the Ctl group, the calvariae were cultured in basal medium, and in the Acid group the calvariae were cultured in medium in which the pH was lowered by the addition of 10 μl HCl/ml medium to lower HCO_3^- concentration ($[HCO_3^-]$). *$P < 0.001$.

as this is the time period during which acidosis induces predominantly cell-mediated bone resorption (9, 11, 30, 31, 40, 48). During more acute acidosis, fewer then 24 h in culture, there is predominantly physicochemical mineral dissolution (24, 36). At the conclusion of the experiments, calvariae were removed from the culture dishes, washed with ice-cold PBS, rapidly frozen in an acetone/dry ice bath (−77°C) for 5 min, and then lyophilized while frozen until dry (at least 16 h) (15–18, 21–23, 28, 34–37). The frontal and parietal bones of some calvariae were split in half to reveal the interior of the bone for cross-sectional analysis. All bones were then mounted on aluminum supports with conductive glue and coated with a thin layer (~5 nm) of gold. This layer, which is rapidly sputtered away by the ion probe from the area being scanned, prevents artifact-inducing electrical charging.

Scanning ion microprobe. The scanning ion microprobe utilized for these studies was conceptualized and built at the University of Chicago and employs a 40-keV gallium beam focused to a spot 40 nm in diameter (15–18, 21–23, 28, 34–37, 53, 54). The beam is scanned across a sample surface in a controlled sequence, resulting in the emission of secondary electrons, ions, and neutral atoms. These secondary particles originate within, and consequently carry information about, the most superficial 1–2 nm of the sample. The charged secondary particles can be collected to generate images of the surface topography of a sample similar to those obtained using a scanning electron microscope. The particles can also be collected and analyzed by SIMS, a technique that separates the sputtered ions according to their mass-to-charge ratio.

In this study, the microanalysis of bone by SIMS was performed in two nonimaging SIMS modes. In the first, the spectrometer is rapidly and sequentially retuned to filter several chosen ion species. At the same time, the probe is quickly scanned over a square area, so that the measured signals are secondary ion intensities averaged over the entire field of view. Using this "peak-switching" technique, the relative concentrations of several elements can be acquired simultaneously from one area and at one sample depth. In the second, a mass analysis mode, the spectrometer mass tuning can be systematically varied (as in a conventional mass spectrometer) to yield mass spectra. If the spectra data are corrected by element-dependent sensitivity factors, they provide quantitative relative abundance measurements for a given area of sample (15–18, 21–23, 28, 34–37, 53, 54).

For SIMS analysis, the secondary ions emerging from the sample are transported through a high-transmission optical system containing an electrostatic energy analyzer and a magnetic sector mass spectrometer (mass resolution of ~0.07 atomic mass unit measured at 40 atomic mass units). The secondary ions are accelerated to 5,000-eV energy for mass separation and detection by a secondary electron detector operated in pulse mode (each collected ion yields 1 digital pulse). Mass spectra are accumulated with a multichannel scaler, which counts each detected ion by ramping the magnetic field of the mass spectrometer to scan a preselected mass region of the spectrum while the probe is scanning an area of arbitrary dimensions. The choice of the scanned area determines the depth over which the target composition is sampled for a given probe current and time. Elemental maps are constructed by recording the individual, detected pulses in a 512 × 512 array of computer memory, each element of the array corresponding to a position of the probe on the sample. For the most abundant elements (sodium, potassium, and calcium), counting rates as high as 4.0×10^5 counts$\cdot s^{-1} \cdot pA^{-1}$ of primary current were observed. In such cases, statistically significant elemental images could be obtained in scan times of <10 s with probe currents of a few tens of picoamperes.

We selected, at random, four calvariae from each group. For each calvaria, we measured the concentration of HCO_3^-, phosphate, carbon-nitrogen bond, and carbon on the surface and on the cross section. The analyses were repeated on six representative areas of each calvaria. Data were recorded after erosion of ~5 nm of material; this procedure ensured the removal of any contamination and permitted the acquisition of highly reproducible measurements and is consistent with our previously published studies (15–18, 21–23, 28, 34–37, 53, 54). Given the beam current of 30 pA and image acquisition time not exceeding 524 s (maximum time in this study), the depth of erosion for these elemental measurements, over areas ranging from 40 × 40 to 160 × 160 μm^2, never exceeded ~5 nm, which did not result in significant sample depletion. Given the extremely small area being examined, 40 × 40 to 160 × 160 μm^2, all cross-sectional measurements were far from the calvarial surface, which is ~1 mm thick.

We compared the ratios of HCO_3^- and total phosphate to the carbon-carbon bond (C_2) and carbon-nitrogen bond (CN). Carbon appears to be a suitable denominator, as it would not be expected to be affected by acid in these relatively short-term experiments. We use C_2 rather than C simply because it gives a stronger signal; the ratio of C_2 to C is constant (Levi-Setti R and Bushinsky DA, unpublished observations). The CN is present in areas of organic material. PO_4 gives a very weak signal, presumably due to the breakup of this large molecule into PO_2 and PO_3 by the gallium beam, and there is little P which is not associated with O. The ratio $[(PO_2 + PO_3)/C_2]$ or $[(PO_2 + PO_3)/CN]$ is not significantly influenced by inclusion of small amounts of PO_4 or P in the numerator (Levi-Setti R and Bushinsky DA, unpublished observations). Carbonate has an atomic mass of 60. Given that mass 60 is also C_5, we would not expect a detectable decrease in mass 60 during metabolic acidosis given the large mass of organic carbon in bone (64), which would not be expected to be affected by acidosis. In contrast HCO_3^- (mass 61), readily accepts hydrogen ions and is a known buffer in the extracellular fluid (10). There are no other common compounds at mass 61, making this an unambiguous marker for bone total CO_2 (carbonate + HCO_3^-). As in previous studies, we have used C_2, CN, total phosphate, and HCO_3^- to study the effects of acid on bone (15, 34). In this study, we do not report positive ions, such as calcium, sodium, and potassium, because we do not know of a standard positive ion or ion cluster, which would not be expected to be influenced by acidosis. We have previously demonstrated that acute acidosis induces a marked loss of bone sodium and potassium in relation to calcium (28). Without a standard for the positive ions, we cannot determine the localization of the loss of sodium and potassium.

Correction methods similar to those that we have previously reported (15–18, 21–23, 28, 34–37, 53, 54) were applied to the observed mass-resolved counting rates to obtain secondary ion yields proportional to the elemental concentration in the sample. Corrections are necessary because of the species-dependent sputtering and ionization probabilities of the emitted atoms. The total ion counts in a micrograph are a function not only of the emission properties of ions from a sample but also of the fraction of the field of view occupied by the sample, which in the case of the calvariae may have physical holes. In addition, the detected ion yields are dependent on the degree of sample surface roughness. Because of these considerations, we express our results in terms of the

ratios of counts obtained for the same area of a sample. Such ratios are independent of the fraction of the field of view occupied by the sample and of the surface topography.

Conventional measurements. Medium pH and P_{CO_2} were determined with a blood-gas analyzer (Radiometer model ABL 30) and calcium by electrode (Nova Biomedical, Waltham, MA). The medium [HCO_3^-] was calculated from medium pH and P_{CO_2} as described previously (8, 11, 25, 36). Net calcium flux was calculated as $V_m([Ca]_f - [Ca]_i)$, where V_m is the medium volume (1.8 ml), and $[Ca]_f$ and $[Ca]_i$ are the final and initial medium calcium concentration, respectively. A positive flux value indicates movement of the ion from the bone into the medium, and a negative value indicates movement from the medium into the bone.

Statistics. All tests of significance were calculated using analysis of variance with a Bonferroni correction for multiple comparisons (BMDP, University of California, Los Angeles, CA) on a digital computer. All values are expressed as means ± SE; $P < 0.05$ was considered significant.

RESULTS

Medium pH, P_{CO_2}, and calcium. Compared with Ctl medium, the initial and final pH and [HCO_3^-] were significantly reduced in the Acid medium during the 0- to 24-h, 24- to 48-h, and 48- to 51-h incubation (Table 1). There were no differences in P_{CO_2} between Ctl and Acid media during any time period. Compared with calvariae incubated in Ctl medium, during each of the three individual incubations and over the entire time period studied, there was a significant increase in net calcium flux from bones incubated in Acid medium (Fig. 1).

HCO_3^-. After 51 h of incubation in Ctl medium, the ratio of HCO_3^- relative to the C_2 bond was greater in the cross section than on the surface of calvariae incubated in Ctl medium; however, the ratio of HCO_3^- relative to the CN bond on the surface was not different from that found on the cross section of calvariae incubated in Ctl medium [Fig. 2, *top*, representative spectra from surface of calvariae in Ctl medium (Control in figure); Fig. 3, *top*, representative spectra from cross section of calvariae in Ctl medium; Fig. 4, *top*, compiled data]. Compared with incubation in Ctl medium, incubation in Acid medium did not alter the ratio of HCO_3^- to C_2 or the ratio of HCO_3^- to CN on the surface of calvariae (Fig. 2, cf. Ctl and Acid and Fig. 4, *top*).

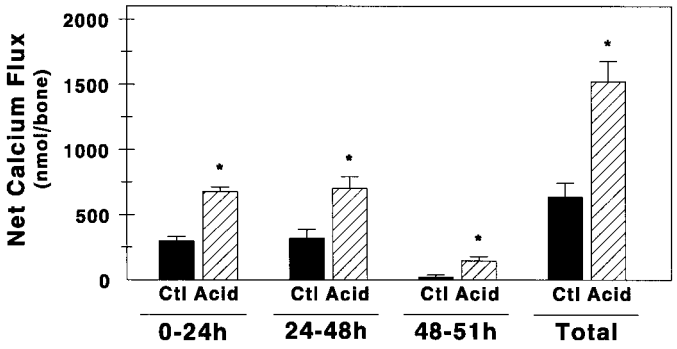

Fig. 1. Net calcium flux from neonatal mouse calvariae incubated in either control (Ctl; initial medium pH ~7.45, HCO_3^- ~26) or acidic (Acid; initial medium pH ~7.14, HCO_3^- ~13) medium for a total of 51 h. Calvariae were transferred to similar fresh preincubated medium at 24 and 48 h. Before and after each incubation, the medium was analyzed for calcium. Total represents the sum of the net calcium flux from the 3 separate incubations in each group. A positive flux represents movement from the bone into the medium. *$P < 0.05$ vs. Ctl.

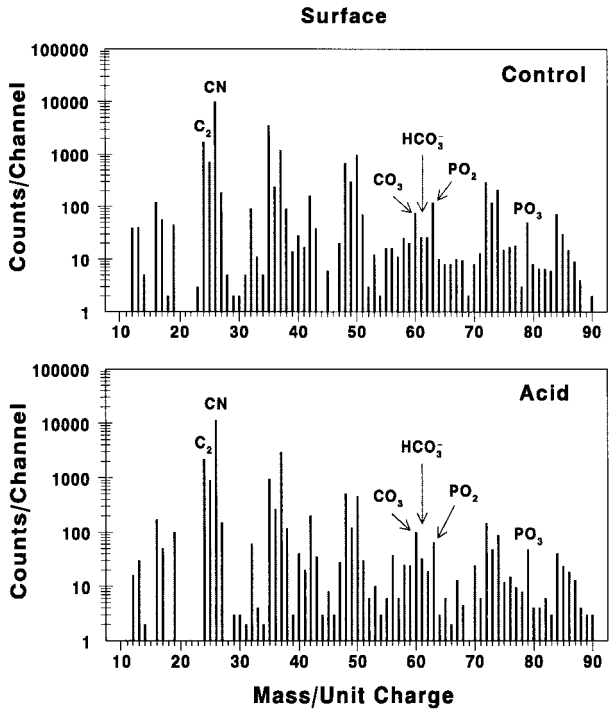

Fig. 2. Mass spectra of the negative secondary ions on the surface of neonatal mouse calvariae incubated for 51 h in either Ctl (Control in figure) or Acid medium. Calvariae were transferred to similar fresh preincubated medium at 24 and 48 h. Counts/channel are counts/s of detected secondary ions uncorrected for species-dependent ionization probabilities. Observed spectra were measured in 1,000 channels equally divided among mass 10–90 atomic mass units. CN, carbon-nitrogen bond; C_2, carbon-carbon bond.

However, compared with incubation in Ctl medium, incubation in Acid medium led to a decrease in the ratio of HCO_3^- to C_2 and a decrease in the ratio of HCO_3^- to CN in the cross section of the calvariae (Fig. 3, cf. Ctl and Acid and Fig. 4, *top*). Thus incubation in Acid medium induces a significant fall in mineral HCO_3^- in the cross section, but not on the surface, of calvariae.

Phosphate. After 51 h of incubation in Ctl medium, the ratio of total phosphate ($PO_2 + PO_3$) relative to C_2 and the ratio of ($PO_2 + PO_3$) relative to CN on the surface were not different from that found on the cross section of calvariae incubated in Ctl medium (Fig. 2, *top*, representative spectra of Ctl surface; Fig. 3, *top*, representative spectra of Ctl cross section; Fig. 4, *bottom*, compiled data). Compared with incubation in Ctl medium, incubation in Acid medium did not alter the ratio of ($PO_2 + PO_3$) to C_2 or the ratio of ($PO_2 + PO_3$) to CN on the surface of calvariae (Fig. 2, cf. Ctl and Acid and Fig. 3, *bottom*).

However, compared with incubation in Ctl medium, incubation in Acid medium led to a decrease in the ratio of ($PO_2 + PO_3$) to C_2 and a decrease in the ratio of

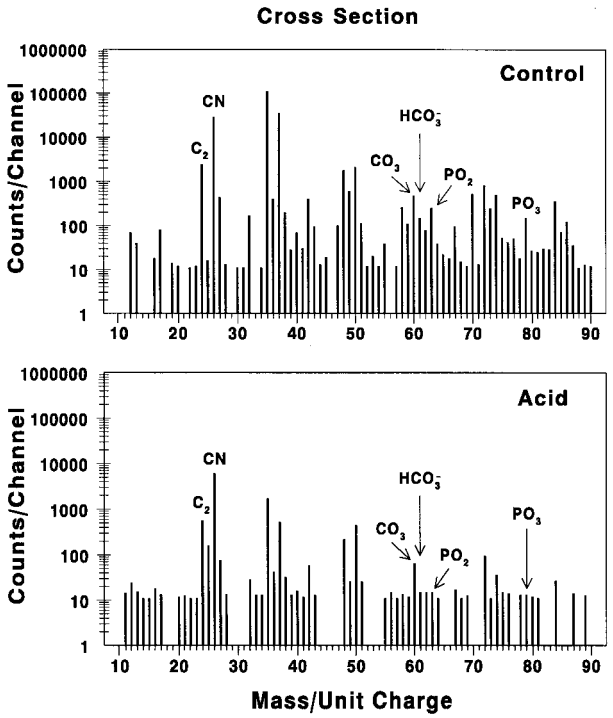

Fig. 3. Mass spectra of the negative secondary ions on a cross section of neonatal mouse calvariae incubated for 51 h in either Ctl or Acid medium. Calvariae were transferred to similar fresh preincubated medium at 24 and 48 h. Counts/channel are counts/s of detected secondary ions uncorrected for species-dependent ionization probabilities. Observed spectra were measured in 1,000 channels equally divided among mass 10–90 atomic mass units.

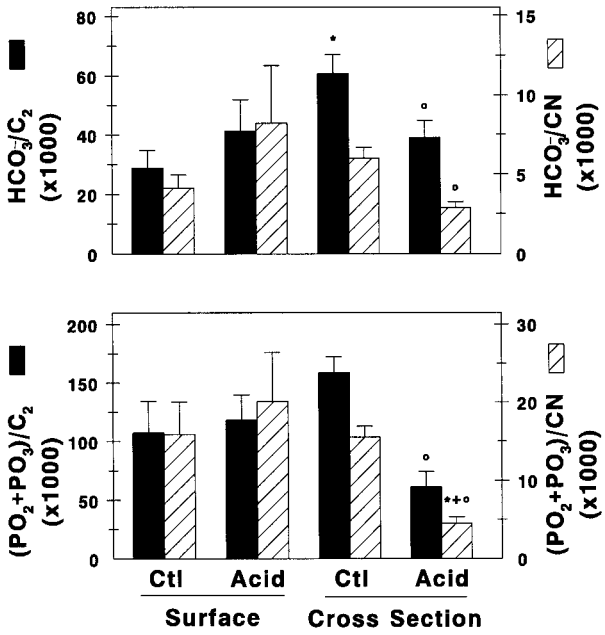

Fig. 4. Ratio of HCO_3^- to the C_2 and ratio of HCO_3^- to the CN on the surface and in the cross section of neonatal mouse calvariae incubated for 51 h in either Ctl or Acid medium (*top*). Calvariae were transferred to similar, fresh preincubated medium at 24 and 48 h. *Bottom*: ratio of total phosphate (PO_2 + PO_3) to C_2 and (PO_2 + PO_3) to CN on the surface and in the cross section of neonatal mouse calvariae incubated for 51 h in either Ctl or Acid medium. Calvariae were transferred to similar fresh preincubated medium at 24 and 48 h. Values are means ± SE. $^*P < 0.05$ vs. surface Ctl; $^+P < 0.05$ vs. surface Acid; $^\circ P < 0.05$ vs. cross-sectional Ctl.

(PO_2 + PO_3) to CN in the cross section of the calvariae (Fig. 3, cf. Ctl and Acid and Fig. 4, *bottom*). Thus incubation in Acid medium induces a significant fall in mineral phosphate in the cross section, but not on the surface, of calvariae.

HCO_3^- in relation to phosphate. The amount of HCO_3^- relative to (PO_2 + PO_3) on the surface of calvariae does not differ significantly from that on the cross section of calvariae incubated in Ctl medium (Fig. 5). Compared with incubation in Ctl medium, incubation in Acid medium did not alter the ratio of HCO_3^- relative to (PO_2 + PO_3) on the surface of the calvariae. However, compared with incubation in Ctl medium, incubation in Acid medium led to a significant increase in the ratio of HCO_3^- to (PO_2 + PO_3) in the cross section of the calvariae. Because incubation in Acid medium led to a reduction of both (PO_2 + PO_3) and HCO_3^- in the cross section of calvariae (Figs. 3 and 4), an increase in the ratio of HCO_3^- to (PO_2 + PO_3) on the cross section of calvariae must indicate depletion of (PO_2 + PO_3) in relation to HCO_3^-. Thus metabolic acidosis induces a fall in mineral (PO_2 + PO_3) in relation to mineral HCO_3^- in the cross section of calvariae.

DISCUSSION

The purpose of the present study was to test the hypothesis that chronic metabolic acidosis would decrease bulk (cross-sectional) bone phosphate to a greater extent than bone carbonate. Using a high-resolution scanning ion microprobe with secondary ion mass spectroscopy, we localized and compared the changes in bone HCO_3^- and phosphate after chronic incubation of neonatal mouse calvariae in acidic medium. We found that compared with bones incubated in a neutral-pH medium, chronic acidosis induced a fall in both cross-sectional HCO_3^- and phosphate with no change in surface HCO_3^- and phosphate and that the fall in phosphate predominated over the fall in HCO_3^-. Consumption of these proton buffers, HCO_3^- and phos-

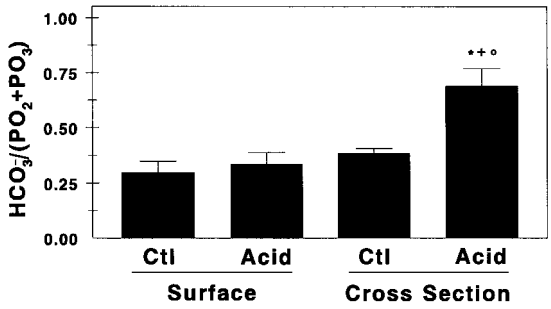

Fig. 5. Ratio of HCO_3^- to (PO_2 + PO_3) on the surface and in the cross section of neonatal mouse calvariae incubated for 51 h in either Ctl or Acid medium. Calvariae were transferred to similar fresh preincubated medium at 24 and 48 h. Values are means ± SE. $^*P < 0.05$ vs. surface Ctl; $^+P < 0.05$ vs. surface Acid; $^\circ P < 0.05$ vs. cross-sectional Ctl.

phate, would help to lessen the fall in pH during chronic acidosis.

We previously studied changes in bulk midcortical ion concentrations after 7 days of in vivo metabolic acidosis induced by oral ammonium chloride (15). We found that compared with mice drinking only distilled water, the ammonium chloride-induced acidosis led to a loss of bone sodium and potassium, and, as also shown in this study, a depletion of mineral HCO_3^- and phosphate. In the previous study, we questioned whether there were regional differences in the response of mineral HCO_3^- and phosphate to chronic metabolic acidosis. The present study clearly demonstrates regional differences in the response of bone to a model of chronic acidosis; the additional protons deplete cross-sectional, but not surface, bone phosphate and carbonate.

We have previously studied the effects of acute acidosis on surface and cross-sectional HCO_3^- and phosphate (34). We found that compared with control, after a 3-h incubation in acidic medium there was a marked decrease in surface HCO_3^- with respect to C_2 and CN with no change in cross-sectional HCO_3^-. Compared with control, after a 3-h incubation in acidic medium, there was also a marked decrease in cross-sectional phosphate with respect to C_2 and also to CN with no change in surface phosphate. On the bone surface, there is a fourfold depletion of HCO_3^- in relation to phosphate and in cross section a sevenfold depletion of phosphate in relation to HCO_3^-. These results indicate that acute H^+ buffering by bone involves preferential dissolution of surface HCO_3^- and of cross-sectional phosphate.

The present study extends the acute observations on bone surface and cross-sectional HCO_3^- and phosphate (34) to a model of chronic acidosis. In the acute study, the surface HCO_3^- fell, whereas in the chronic study there was no change in surface HCO_3^-. However, in the acute study the control surface HCO_3^- was higher than the control surface HCO_3^- in this chronic study, suggesting that 51 h of culture in control medium may have led to a depletion in surface HCO_3^-. Perhaps the surface HCO_3^- is buffering the acids generated through normal cellular metabolism. Indeed, the medium HCO_3^- fell by the end of the two 48-h incubations of the control bones (Table 1). In the acute study, there was no change in surface phosphate, similar to the results of this study, and the levels of phosphate in the two studies were comparable. In the acute study, there was no change in cross-sectional HCO_3^-, whereas in this chronic study the cross-sectional HCO_3^- fell. This suggests that with time the cross-sectional HCO_3^- is depleted by acidosis in the process of buffering the additional hydrogen ions. In the acute study, the acidic medium resulted in a marked fall in cross-sectional phosphate, as also occurred in this chronic study. Taken together, the results of the two studies suggest that the surface of the control bone cultured for 3 h is rich in HCO_3^- and the cross section is rich in phosphate. An acidic medium rapidly depletes the surface HCO_3^- and cross-sectional phosphate. With more prolonged incubation in acidic medium, the cross-sectional, but not the surface, phosphate and HCO_3^- are further depleted. The consumption of these proton buffers during incubation in acidic medium helps to mitigate the fall in pH.

That the acid-induced depletion of phosphate would predominate over the depletion of HCO_3^- in a chronic study of neonatal mouse bone is not unexpected. Using Raman vibrational microspectroscopy, Tarnowski et al. (63) found that the ratio of carbonate to phosphate in mouse calvariae 3 and 7 days postnatal is ~0.12, indicating that there is far more phosphate than HCO_3^- available as a potential proton buffer. Each released PO_4 would accept a proton in the ratio of four HPO_4^{2-} to one $H_2PO_4^-$ at pH 7.4. The lower the pH, the greater the ratio of $H_2PO_4^-$ in relation to HPO_4^{2-}. Bone CO_3^{2-} would combine with H^+ to form HCO_3^- and then with an additional H^+ to form H_2CO_3, which rapidly dissociates to H_2O and CO_2.

Other studies have shown that during in vitro (7, 8, 25, 28) and in vivo (51, 59, 62) metabolic acidosis, the mineral phases of bone appear to buffer some of the additional protons, resulting in an increase in medium or systemic pH, respectively (10, 14, 20). In cultured bone, we have previously shown that an acute reduction of medium pH is associated with an influx of H^+ into the bone (7, 8, 25), an efflux of sodium and potassium from bone (22, 22, 28, 36, 37), and a loss of mineral carbonate (26, 27). The sodium and potassium exchange for H^+ decreases the ambient H^+ concentration. Because the majority of bone consists of calcium phosphate complexes, the acid-induced, cell-mediated bone resorption that occurs during chronic metabolic acidosis (11, 22, 30, 48) would result in the release of mineral phosphate. We and others have shown a loss of bone carbonate during metabolic acidosis (4, 30), and we have shown that in vivo metabolic acidosis causes a reduction in mineral HCO_3^- and phosphate (15).

Clinical observations in patients with renal tubular acidosis support the hypothesis that acidosis has deleterious effects on bone mineral. Metabolic acidosis has been shown to have a significant effect on bone density, formation, and growth (38, 39, 55, 56). Domrongkitchaiporn and co-workers (38) compared 14 adult patients with distal renal tubular acidosis who had never received HCO_3^- therapy with 28 well-matched controls. They measured bone mineral density and also performed bone biopsies with histomorphometric analysis (38). They found that patients with distal renal tubular acidosis had a lower bone mineral density in most areas compared with normal controls. The patients also had a decreased bone formation rate. After treating 12 renal tubular acidosis patients with $KHCO_3$ for 1 yr, they found that bone mineral density significantly improved in the trochanter of the femur and the total femur (39). The bone formation rate normalized with treatment. Initially, the levels of serum parathyroid hormone were suppressed; they too improved with $KHCO_3$ therapy (38, 39). McSherry and Morris (55, 56) studied the effect of renal tubular acidosis on growth in 10 children. Six were found to be

stunted (height <2.5 SD), two were too young to determine whether they were short (<2 wk old), and two were previously not acidemic. With sustained alkali therapy, each patient attained and maintained normal stature, mean height increased from the 1.4 to the 37th percentile, and the rate of growth increased two- to threefold.

The results of the present study are consistent with those of previous investigators. In a classic study, Swann and Pitts (62) infused fixed amounts of acid into dogs and demonstrated that ~60% of the additional protons appear to be buffered outside of the extracellular fluid, presumably by soft tissues (1, 57) and/or bone (5, 51). In vivo, Irving and Chute (45) demonstrated that several days of metabolic acidosis led to a loss of bone carbonate. Burnell (6) also demonstrated a loss of bone carbonate after metabolic acidosis, and Bettice (4, 5) showed that the metabolic acidosis-induced loss of bone carbonate correlated with the fall in extracellular HCO_3^-. Using cultured neonatal mouse calvariae, we demonstrated that mineral calcium and carbonate, in the form of carbonated apatite, are in equilibrium with the culture medium (27). We have shown that acidosis induces the release of calcium and carbonate from bone (27), leading to a progressive loss of bone carbonate during metabolic, but not respiratory, acidosis (26).

In the present study, we used a high-resolution scanning ion microprobe with secondary ion mass spectroscopy to localize the changes in bone HCO_3^- and phosphate in response to a model of chronic metabolic acidosis. We found that chronic acidosis induced a fall in both cross-sectional HCO_3^- and phosphate with no change in surface HCO_3^- and phosphate and that the fall in phosphate predominated over the fall in HCO_3^-. Consumption of these proton buffers, HCO_3^- and phosphate, would help to lessen the fall in pH during chronic acidosis at the expense of the bone mineral content.

DISCLOSURES

This work was supported in part by National Institutes of Health Grants AR-46289 and DK-56788.

REFERENCES

1. **Adler S, Roy A, and Relman AS.** Intracellular acid-base regulation. I. The response of muscle cells to changes in CO_2 tension or extracellular bicarbonate concentration. *J Clin Invest* 44: 8–20, 1965.
2. **Barzel US.** The effect of excessive acid feeding on bone. *Calcif Tissue Res* 4: 94–100, 1969.
3. **Barzel US.** The skeleton as an ion exchange system: implications for the role of acid-base imbalance in the genesis of osteoporosis. *J Bone Miner Res* 10: 1431–1436, 1995.
4. **Bettice JA.** Skeletal carbon dioxide stores during metabolic acidosis. *Am J Physiol Renal Fluid Electrolyte Physiol* 247: F326–F330, 1984.
5. **Bettice JA and Gamble JL Jr.** Skeletal buffering of acute metabolic acidosis. *Am J Physiol* 229: 1618–1624, 1975.
6. **Burnell JM.** Changes in bone sodium and carbonate in metabolic acidosis and alkalosis in the dog. *J Clin Invest* 50: 327–331, 1971.
7. **Bushinsky DA.** Effects of parathyroid hormone on net proton flux from neonatal mouse calvariae. *Am J Physiol Renal Fluid Electrolyte Physiol* 252: F585–F589, 1987.
8. **Bushinsky DA.** Net proton influx into bone during metabolic, but not respiratory, acidosis. *Am J Physiol Renal Fluid Electrolyte Physiol* 254: F306–F310, 1988.
9. **Bushinsky DA.** Net calcium efflux from live bone during chronic metabolic, but not respiratory, acidosis. *Am J Physiol Renal Fluid Electrolyte Physiol* 256: F836–F842, 1989.
10. **Bushinsky DA.** Metabolic acidosis. In: *The Principles and Practice of Nephrology*, edited by Jacobson HR, Striker GE, and Klahr S. St. Louis, MO: Mosby, 1995, p. 924–932.
11. **Bushinsky DA.** Stimulated osteoclastic and suppressed osteoblastic activity in metabolic but not respiratory acidosis. *Am J Physiol Cell Physiol* 268: C80–C88, 1995.
12. **Bushinsky DA.** The contribution of acidosis to renal osteodystrophy. *Kidney Int* 47: 1816–1832, 1995.
13. **Bushinsky DA.** Metabolic alkalosis decreases bone calcium efflux by suppressing osteoclasts and stimulating osteoblasts. *Am J Physiol Renal Fluid Electrolyte Physiol* 271: F216–F222, 1996.
14. **Bushinsky DA.** Acid-base imbalance and the skeleton. *Eur J Nutr* 40: 238–244, 2001.
15. **Bushinsky DA, Chabala JM, Gavrilov KL, and Levi-Setti R.** Effects of in vivo metabolic acidosis on midcortical bone ion composition. *Am J Physiol Renal Physiol* 277: F813–F819, 1999.
16. **Bushinsky DA, Chabala JM, and Levi-Setti R.** Ion microprobe analysis of bone surface elements: effects of $1,25(OH)_2D_3$. *Am J Physiol Endocrinol Metab* 257: E815–E822, 1989.
17. **Bushinsky DA, Chabala JM, and Levi-Setti R.** Ion microprobe analysis of mouse calvariae in vitro: evidence for a "bone membrane." *Am J Physiol Endocrinol Metab* 256: E152–E158, 1989.
18. **Bushinsky DA, Chabala JM, and Levi-Setti R.** Comparison of in vitro and in vivo ^{44}Ca labeling of bone by scanning ion microprobe. *Am J Physiol Endocrinol Metab* 259: E586–E592, 1990.
19. **Bushinsky DA, Favus MJ, Schneider AB, Sen PK, Sherwood LM, and Coe FL.** Effects of metabolic acidosis on PTH and $1,25(OH)_2D_3$ response to low calcium diet. *Am J Physiol Renal Fluid Electrolyte Physiol* 243: F570–F575, 1982.
20. **Bushinsky DA and Frick KK.** The effects of acid on bone. *Curr Opin Nephrol Hypertens* 9: 369–379, 2000.
21. **Bushinsky DA, Gavrilov K, Chabala JM, Featherstone JDB, and Levi-Setti R.** Effect of metabolic acidosis on the potassium content of bone. *J Bone Miner Res* 12: 1664–1671, 1997.
22. **Bushinsky DA, Gavrilov K, Stathopoulos VM, Krieger NS, Chabala JM, and Levi-Setti R.** Effects of osteoclastic resorption on bone surface ion composition. *Am J Physiol Cell Physiol* 271: C1025–C1031, 1996.
23. **Bushinsky DA, Gavrilov KL, Chabala JM, and Levi-Setti R.** Contribution of organic material to the ion composition of bone. *J Bone Miner Res* 15: 2026–2032, 2000.
24. **Bushinsky DA, Goldring JM, and Coe FL.** Cellular contribution to pH-mediated calcium flux in neonatal mouse calvariae. *Am J Physiol Renal Fluid Electrolyte Physiol* 248: F785–F789, 1985.
25. **Bushinsky DA, Krieger NS, Geisser DI, Grossman EB, and Coe FL.** Effects of pH on bone calcium and proton fluxes in vitro. *Am J Physiol Renal Fluid Electrolyte Physiol* 245: F204–F209, 1983.
26. **Bushinsky DA, Lam BC, Nespeca R, Sessler NE, and Grynpas MD.** Decreased bone carbonate content in response to metabolic, but not respiratory, acidosis. *Am J Physiol Renal Fluid Electrolyte Physiol* 265: F530–F536, 1993.
27. **Bushinsky DA and Lechleider RJ.** Mechanism of proton-induced bone calcium release: calcium carbonate-dissolution. *Am J Physiol Renal Fluid Electrolyte Physiol* 253: F998–F1005, 1987.
28. **Bushinsky DA, Levi-Setti R, and Coe FL.** Ion microprobe determination of bone surface elements: effects of reduced medium pH. *Am J Physiol Renal Fluid Electrolyte Physiol* 250: F1090–F1097, 1986.

29. **Bushinsky DA and Monk RD.** Calcium. *Lancet* 352: 306–311, 1998.
30. **Bushinsky DA and Nilsson EL.** Additive effects of acidosis and parathyroid hormone on mouse osteoblastic and osteoclastic function. *Am J Physiol Cell Physiol* 269: C1364–C1370, 1995.
31. **Bushinsky DA, Parker WR, Alexander KM, and Krieger NS.** Metabolic, but not respiratory, acidosis increases bone PGE_2 levels and calcium release. *Am J Physiol Renal Physiol* 281: F1058–F1066, 2001.
32. **Bushinsky DA and Sessler NE.** Critical role of bicarbonate in calcium release from bone. *Am J Physiol Renal Fluid Electrolyte Physiol* 263: F510–F515, 1992.
33. **Bushinsky DA, Sessler NE, and Krieger NS.** Greater unidirectional calcium efflux from bone during metabolic, compared with respiratory, acidosis. *Am J Physiol Renal Fluid Electrolyte Physiol* 262: F425–F431, 1992.
34. **Bushinsky DA, Smith SB, Gavrilov KL, Gavrilov LF, Li J, and Levi-Setti R.** Acute acidosis-induced alteration in bone bicarbonate and phosphate. *Am J Physiol Renal Physiol* 283: F1091–F1097, 2002.
35. **Bushinsky DA, Sprague S, Hallegot P, Girod C, Chabala JM, and Levi-Setti R.** Effects of aluminum on bone surface ion composition. *J Bone Miner Res* 10: 1988–1997, 1995.
36. **Bushinsky DA, Wolbach W, Sessler NE, Mogilevsky R, and Levi-Setti R.** Physicochemical effects of acidosis on bone calcium flux and surface ion composition. *J Bone Miner Res* 8: 93–102, 1993.
37. **Chabala JM, Levi-Setti R, and Bushinsky DA.** Alteration in surface ion composition of cultured bone during metabolic, but not respiratory, acidosis. *Am J Physiol Renal Fluid Electrolyte Physiol* 261: F76–F84, 1991.
38. **Domrongkitchaiporn S, Pongsakul C, Stitchantrakul W, Sirikulchayanonta V, Ongphiphadhanakul B, Radinahamed P, Karnsombut P, Kunkitti N, Ruang-raksa C, and Rajatanavin R.** Bone mineral density and histology in distal renal tubular acidosis. *Kidney Int* 59: 1086–1093, 2001.
39. **Domrongkitchaiporn S, Pongskul C, Sirikulchayanonta V, Stitchantrakul W, Leeprasert V, Ongphiphadhanakul B, Radinahamed P, and Rajatanavin R.** Bone histology and bone mineral density after correction of acidosis in distal renal tubular acidosis. *Kidney Int* 62: 2160–2166, 2002.
40. **Frick KK and Bushinsky DA.** Chronic metabolic acidosis reversibly inhibits extracellular matrix gene expression in mouse osteoblasts. *Am J Physiol Renal Physiol* 275: F840–F847, 1998.
41. **Frick KK and Bushinsky DA.** In vitro metabolic and respiratory acidosis selectively inhibit osteoblastic matrix gene expression. *Am J Physiol Renal Physiol* 277: F750–F755, 1999.
42. **Frick KK, Jiang L, and Bushinsky DA.** Acute metabolic acidosis inhibits the induction of osteoblastic *egr*-1 and type 1 collagen. *Am J Physiol Cell Physiol* 272: C1450–C1456, 1997.
43. **Gafter U, Kraut JA, Lee DBN, Silis V, Walling MW, Kurokawa K, Haussler MR, and Coburn JW.** Effect of metabolic acidosis in intestinal absorption of calcium and phosphorus. *Am J Physiol Gastrointest Liver Physiol* 239: G480–G484, 1980.
44. **Goldhaber P and Rabadjija L.** H^+ stimulation of cell-mediated bone resorption in tissue culture. *Am J Physiol Endocrinol Metab* 253: E90–E98, 1987.
45. **Irving L and Chute AL.** The participation of carbonates of bone in the neutralization of ingested acid. *J Cell Comp Physiol* 2: 157–176, 1932.
46. **Krieger NS, Frick KK, and Bushinsky DA.** Cortisol inhibits acid-induced bone resorption in-vitro. *J Am Soc Nephrol* 13: 2534–2539, 2002.
47. **Krieger NS, Parker WR, Alexander KM, and Bushinsky DA.** Prostaglandins regulate acid-induced cell-mediated bone resorption. *Am J Physiol Renal Physiol* 279: F1077–F1082, 2000.
48. **Krieger NS, Sessler NE, and Bushinsky DA.** Acidosis inhibits osteoblastic and stimulates osteoclastic activity in vitro. *Am J Physiol Renal Fluid Electrolyte Physiol* 262: F442–F448, 1992.
49. **Lemann J Jr, Adams ND, and Gray RW.** Urinary calcium excretion in human beings. *N Engl J Med* 301: 535–541, 1979.
50. **Lemann J Jr, Adams ND, Wilz DR, and Brenes LG.** Acid and mineral balances and bone in familial proximal renal tubular acidosis. *Kidney Int* 58: 1267–1277, 2000.
51. **Lemann J Jr, Litzow JR, and Lennon EJ.** The effects of chronic acid loads in normal man: further evidence for the participation of bone mineral in the defense against chronic metabolic acidosis. *J Clin Invest* 45: 1608–1614, 1966.
52. **Lemann J Jr, Litzow JR, and Lennon EJ.** Studies of the mechanism by which chronic metabolic acidosis augments urinary calcium excretion in man. *J Clin Invest* 46: 1318–1328, 1967.
53. **Levi-Setti R and LeBeau M.** Cytogenetic applications of high resolution secondary ion imaging microanalysis: detection and mapping of tracer isotopes in human chromosomes. *Biol Cell* 74: 51–58, 1992.
54. **Lundgren T, Engstrom EU, Levi-Setti R, Linde A, and Noren JG.** The use of the stable isotope ^{44}Ca in studies of calcium incorporation into dentin. *J Microsc* 173: 149–154, 1994.
55. **McSherry E.** Acidosis and growth in nonuremic renal disease. *Kidney Int* 14: 349–354, 1978.
56. **McSherry E and Morris RC.** Attainment and maintenance of normal stature with alkali therapy in infants and children with classic renal tubular acidosis. *J Clin Invest* 61: 509–527, 1978.
57. **Poole-Wilson PA and Cameron IR.** Intracellular pH and K^+ of cardiac and skeletal muscle in acidosis and alkalosis. *Am J Physiol* 229: 1305–1310, 1975.
58. **Rabadjija L, Brown EM, Swartz SL, Chen CJ, and Goldhaber P.** H^+-stimulated release of prostaglandin E_2 and cyclic adenosine 3′, 5′-monophosphoric acid and their relationship to bone resorption in neonatal mouse calvaria cultures. *Bone Miner* 11: 295–304, 1990.
59. **Schwartz WB and Relman AS.** Acidosis in renal disease. *N Engl J Med* 256: 1184–1186, 1957.
60. **Sprague SM, Krieger NS, and Bushinsky DA.** Greater inhibition of in vitro bone mineralization with metabolic than respiratory acidosis. *Kidney Int* 46: 1199–1206, 1994.
61. **Sutton RAL, Wong NLM, and Dirks JH.** Effects of metabolic acidosis and alkalosis on sodium and calcium transport in the dog kidney. *Kidney Int* 15: 520–533, 1979.
62. **Swan RC and Pitts RF.** Neutralization of infused acid by nephrectomized dogs. *J Clin Invest* 34: 205–212, 1955.
63. **Tarnowski CP, Ignelzi MA Jr, and Morris MD.** Mineralization of developing mouse calvaria as revealed by raman microspectroscopy. *J Bone Miner Res* 17: 1118–1126, 2002.
64. **Widdowson EM and Dickerson JWT.** Chemical composition of the body. In: *Mineral Metabolism*, edited by Comar CL and Bronner F. New York: Academic, 1964, p. 1–247.